

Interrelation between Drop Size and Protein Adsorption at Various Emulsification Conditions

Slavka Tcholakova,[†] Nikolai D. Denkov,^{*,†} Doroteya Sidzhakova,[†]
Ivan B. Ivanov,[†] and Bruce Campbell[‡]

Laboratory of Chemical Physics & Engineering, Faculty of Chemistry, Sofia University,
1164 Sofia, Bulgaria, and Kraft Foods Incorporated, 801 Waukegan Road,
Glenview, Illinois 60025

Received March 10, 2003. In Final Form: May 13, 2003

A systematic study of the dependence of mean drop diameter, d_{32} , and protein adsorption, Γ , on (1) whey protein concentration and (2) hydrodynamic conditions during emulsification is performed with soybean-oil-in-water emulsions. We find experimentally and explain theoretically an interesting interplay between Γ and d_{32} in the studied systems: At low protein concentrations, the mean drop size is governed by a critical value of the protein adsorption, Γ^* , which is a characteristic of the emulsifier and does not depend on the hydrodynamic conditions. On the other hand, at higher protein concentrations, Γ is determined by the initial protein concentration in the aqueous phase, C_{PR}^{INI} , and by the mean drop size, d_{32} , the latter being governed only by the hydrodynamic conditions. The theoretical model, developed to describe these relations, is verified by comparing its predictions with experimental results obtained at various protein concentrations, oil volume fractions, and hydrodynamic conditions. The model allows one to predict the dependence of various, technologically important quantities on the emulsification conditions.

1. Introduction

The final drop size distribution obtained after an emulsification process is a result of dynamic equilibrium between drop breakage and drop–drop coalescence; in fact, both processes are promoted by the intense agitation during emulsion formation.^{1,2} The evolution of the drop size distribution in an agitated emulsion depends on many variables related to emulsification conditions (equipment, duration, temperature, etc.) and to the nature and concentration of the emulsifier (kinetics of adsorption, interfacial tension, etc.), which in turn determine the drop–drop interaction and the barrier to coalescence.

A detailed discussion of various factors that affect emulsification is presented by Walstra.^{1,3,4} Theoretical analysis and results from emulsification experiments show that in a turbulent flow and excess of emulsifier, the mean drop diameter should depend on the average power density of energy dissipation in the emulsification chamber, as well as on the density of the aqueous phase and the interfacial tension (see section 3.2 below for more details). Phipps⁵ developed a theoretical model that relates the mean drop size to the mechanical operating characteristics of the poppet valve in a high-pressure homogenizer and

to the emulsion viscosity. This model was found to describe a large set of experimental data.⁵ As mentioned above, these studies considered the case when the equilibrium drop diameter is determined primarily by the hydrodynamic conditions, when the emulsifier is in an excess in the aqueous phase (so-called “surfactant-rich regime”⁶).

On the other hand, at lower emulsifier concentrations, the mean drop size strongly depends on the type of emulsifier and its initial concentration.^{2,6–12} It was experimentally shown in refs 2 and 6–12 (with various surfactants and under different hydrodynamic conditions during emulsification) that the mean drop size significantly decreased with the increase of the initial emulsifier concentration. Oil transfer experiments, performed by Taisne et al.,⁶ Lobo,¹³ and Danner and Schubert,¹⁴ proved that extensive recoalescence took place during emulsification in this surfactant-poor regime. In contrast, in the surfactant-rich regime, the rate of recoalescence of the newly formed drops during emulsification was found to be rather low.⁶ The rate constants of the drop–drop coalescence during emulsification were measured by various techniques in refs 2, 6, 7, and 14.

* To whom correspondence should be addressed. Mail: Assoc. Prof. Nikolai Denkov, Laboratory of Chemical Physics & Engineering, Faculty of Chemistry, Sofia University, 1 James Bourchier Ave., 1164 Sofia, Bulgaria. Phone: (+359-2) 962 5310. Fax: (+359-2) 962 5643. E-mail: ND@LCPE.UNI-SOFIA.BG.

[†] Sofia University.

[‡] Kraft Foods Inc.

(1) Walstra, P. Formation of emulsions. In *Encyclopedia of Emulsion Technology*; Marcel Dekker: New York, 1983; Chapter 2.

(2) Narsimhan, G.; Goel, P. Drop coalescence during emulsion formation in a high-pressure homogenizer for tetradecane-in-water emulsion stabilized by sodium dodecyl sulfate. *J. Colloid Interface Sci.* **2001**, *238*, 420.

(3) Walstra, P.; Smulders, P. Formation of emulsions. In *Proceedings of the 1st World Congress on Emulsions*, Paris, France, 1993; EDS Editeur: Paris, 1993.

(4) Walstra, P.; Geurts, T. J.; Noomen, A.; Jellema, A.; van Boekel, M. A. J. S. *Dairy Technology*; Marcel Dekker: New York, 1999.

(5) Phipps, L. W. The fragmentation of oil drops in emulsions by a high-pressure homogenizer. *J. Phys. D: Appl. Phys.* **1975**, *8*, 448.

(6) Taisne, L.; Walstra, P.; Cabane, B. Transfer of oil between emulsion droplets. *J. Colloid Interface Sci.* **1996**, *184*, 378.

(7) Mohan, S.; Narsimhan, G. Coalescence of protein-stabilized emulsions in a high-pressure homogenizer. *J. Colloid Interface Sci.* **1997**, *192*, 1.

(8) Das, K. P.; Kinsella, J. E. Droplet size and coalescence stability of whey protein stabilized milkfat peanut oil emulsions. *J. Food Sci.* **1993**, *58*, 439.

(9) Gopal, E. S. R. Principles of emulsion formation. In *Emulsion Science*; Sherman, P., Ed.; Academic Press: London, 1968.

(10) Euston, S. R.; Hirst, R. L.; Hill, J. P. The emulsifying properties of β -lactoglobulin genetic variants A, B and C. *Colloids Surf.* **1999**, *12*, 193.

(11) Djakovic, L.; Dokic, P.; Radivojevic, P.; Sefer, I.; Sovilj, V. Action of emulsifiers during homogenization of o/w emulsions. *Colloid Polym. Sci.* **1987**, *265*, 993.

(12) van Aken, G. A.; Zoet, F. D. Coalescence in highly concentrated emulsions. *Langmuir* **2000**, *16*, 7131.

(13) Lobo, L. Coalescence during emulsification: 3. Effect of gelatin on rupture and coalescence. *J. Colloid Interface Sci.* **2002**, *254*, 165.

(14) Danner, T.; Schubert, H. Coalescence processes in emulsions. In *Food Colloids 2000, Fundamentals of Formulation*; Dickinson, E., Miller, R., Eds.; Royal Society of Chemistry: Cambridge, 2001; p 116.

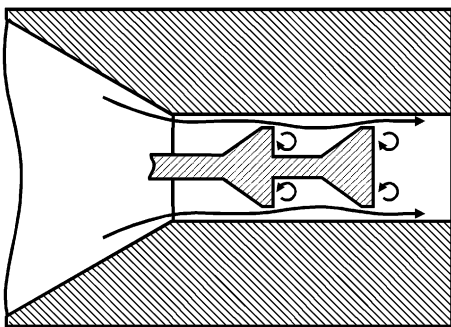


Figure 1. Schematic presentation of the shape of the processing element in the used narrow-gap homogenizer.

Recently, we showed experimentally¹⁵ that oil-in-water emulsions, stabilized by β -lactoglobulin (BLG), could be obtained only if the protein adsorption on the drop surface was above a certain threshold value, $\Gamma^* \approx 1.55 \text{ mg/m}^2$, which was very close to the value for a dense monolayer of BLG molecules, $\Gamma_M \approx 1.65 \text{ mg/m}^2$. This result was obtained at several different protein concentrations in the aqueous phase under fixed hydrodynamic conditions during emulsification.

In the present study, we extend our previous work¹⁵ by performing a systematic investigation of the effect of emulsifier concentration on the mean drop size and on protein adsorption in both protein-poor and protein-rich regimes. The hydrodynamic conditions during emulsification are also varied in the present work to evaluate their effect on the studied quantities. We find experimentally and explain theoretically an interesting interplay between protein adsorption and drop size in the studied systems. The suggested theoretical model is verified by comparing its predictions with experimental results, obtained at various protein concentrations, hydrodynamic conditions, and oil volume fractions. The model allows one to predict the dependence of various, technologically important quantities on the emulsification conditions.

2. Materials and Methods

2.1. Materials. Whey protein concentrate (WPC; trade name AMP8000; product of Proliant) was used as the emulsifier in these experiments. According to the certificate of AMP8000, this protein concentrate of technical grade contains 71.7 wt % proteins, 17.2 wt % carbohydrates, 6.2 wt % water, 2.8 wt % ash, and 2.1 wt % fat. The protein content of WPC includes 44 wt % BLG, 24 wt % α -lactalbumin, 5 wt % bovine serum albumin, and 27 wt % of other proteins. Soybean oil (SBO) was used as an oil phase, which was purified from polar contaminants by passing it through a glass column filled with Florisil adsorbent.¹⁶ The aqueous solutions were prepared with deionized water, purified by a Milli-Q Organex system (Millipore). Along with the protein concentrate, all solutions contained 0.15 M NaCl (Merck, analytical grade, heated for 5 h at 450 °C) and 0.01 wt % of the antibacterial agent NaN_3 (Riedel-de Haën). The experiments were carried out at the natural pH ≈ 6.2 for WPC solutions, without additional adjustment.

2.2. Emulsion Preparation. Oil-in-water emulsions were prepared by using a two-step procedure. Initially, an oil-in-water premix was prepared by hand-shaking of a vessel containing the necessary amounts of oil and protein solution (depending on the desired oil volume fraction in the final emulsion). The second homogenization step was accomplished by passing this premix through the slits of a narrow-gap homogenizer. The mixing head of this homogenizer has a processing element (see Figure 1),

(15) Tcholakova, S.; Denkov, N. D.; Ivanov, I. B.; Campbell, B. Coalescence in β -lactoglobulin-stabilized emulsions: effects of protein adsorption and drop size. *Langmuir* **2002**, *18*, 8960.

(16) Gaonkar, G.; Borwankar, R. P. Competitive adsorption of monoglycerides and lecithin at the vegetable oil-water interface. *Colloids Surf.* **1991**, *59*, 331.

Table 1. Applied Pressure at the Inlet of the Homogenizer (p), Flow Rate (Q), Mixing Time, Oil Volume Fraction (Φ), Geometrical Volume of the Slit (V_S), and Number of Mixture Passes through the Homogenizer for the Used Processing Elements

gap width of the processing element, μm	applied pressure, Pa	flow rate, L/s	mixing time, min	Φ	$V_S \times 10^9, \text{m}^3$	number of passes
75	5×10^5	0.057	2	0.28	2.4	10
195	5×10^5	0.080	5	0.28	8.8	35
295	3.2×10^5	0.115	10	0.28	13.1	100
395	2.2×10^5	0.130	10	0.15	17.2	110
				0.28		
				0.45		

which ensures the passing of the oil-water mixture through two consecutive slits under a moderate pressure, in the range between 2.2×10^5 and 5×10^5 Pa in our experiments. Four different processing elements, with the gap width falling in the range between 75 and 395 μm , were used to study the influence of the hydrodynamic conditions during emulsification on the mean drop size and on the protein adsorption in the produced emulsions. A closed loop (i.e., circulation of the mixture) was used to ensure multiple passes of the oil-water mixture through the homogenizer. The applied pressure at the inlet of the homogenizer, the flow rate, the emulsification duration, and the corresponding number of passes of the emulsion through the homogenizer are presented in Table 1 for the used processing elements. The duration of emulsification was chosen in such a way that the emulsion temperature was 26 ± 1 °C at the end of the process; the reason was that the protein adsorption depended on temperature (see section 3.8 and Table 3 below), and we wanted to exclude this factor from our study. As shown in section 3.1 below, the chosen duration of the emulsification procedure was sufficient for reaching the steady state of the drop size distribution.

2.3. Determination of Drop Size Distribution. The drop size distribution in the emulsions was determined by optical microscopy. The oil drops were observed in transmitted light with microscope Axioplan (Zeiss, Germany), equipped with objective Epiplan $\times 50$ and connected to a CCD camera (Sony) and video recorder (Samsung SV-4000). The diameters of the recorded oil drops were measured (one by one) by using a custom-made image analysis software operating with a Targa+ graphics board (Truevision, USA). The diameters of at least 10^4 drops (from 2–5 independently prepared emulsions) were measured for each system.

The mean volume-surface diameter, d_{32} , was calculated from the size distribution histogram by using the relation

$$d_{32} = \frac{\sum N_i d_i^3}{\sum N_i d_i^2} \quad (1)$$

where N_i is the number of drops with diameter d_i . One can calculate the specific surface area of the drops, S (area per unit volume of dispersed oil), from d_{32} by the equation

$$S = \frac{6}{d_{32}} \quad (2)$$

2.4. Determination of Protein Adsorption. The protein adsorption was calculated from the specific surface area of the oil drops, S , and from the decrease of protein concentration in the aqueous phase as a result of the emulsification process, ΔC_{PR} .

The protein concentration in the aqueous phase was determined by the method of Bradford¹⁷ under the assumption that all proteins in WPC react with the colored reagent of Bradford, causing one and the same spectral shift of the reagent. This assumption is supported by the experimental results of Bradford,¹⁷ who observed a very slight dependence of the spectral shift of the protein-dye mixture on protein type. Our own

(17) Bradford, M. A rapid and sensitive method for the quantitation of microgram quantities of protein utilizing the principle of protein-dye binding. *Anal. Biochem.* **1976**, *72*, 248.

experiments confirmed that the result of the Bradford reaction practically did not depend on the type of used protein (we tested WPC, as well as β -lactoglobulin, α -lactalbumin, and bovine serum albumin, which are the main protein constituents of WPC).

Briefly, the experimental procedure for determination of protein adsorption was the following: After preparing the emulsions, they were kept immobile in a gravity field for 30 min. During this period, the oil drops floated up under the action of buoyancy, forming a cream. The serum remaining below the cream was taken out from the vial by using a syringe. At this stage, the serum was slightly turbid, because it contained a small fraction of dispersed tiny oil drops. To remove these drops, which could affect the protein concentration determination, the serum was centrifuged for 1 h at 4500 rpm and the lower half of the serum (deprived of drops) was used for further analysis. The protein concentration in the serum was determined by the method of Bradford¹⁷ by using a UV-vis spectrophotometer (UNICAM 5625) at a light wavelength of 595 nm. Two calibration curves were prepared from protein solutions of known concentrations, which were passed through the homogenization device and centrifuged (under the same conditions as those described above for the studied emulsions and serums) before mixing with the Bradford reagent: If the protein concentration in the aqueous phase was between 10 and 100 $\mu\text{g/mL}$, 100 μL of the protein solution was mixed with 5 mL of the dye solution; alternatively, if the protein concentration was between 1 and 10 $\mu\text{g/mL}$, 500 μL of the protein solution was mixed with 5 mL of the dye solution (so-called microprotein assay¹⁷). The appropriate calibration curve was used, depending on the protein concentration in the serum, $C_{\text{PR}}^{\text{SER}}$. From the latter value and the mean volume-surface diameter, d_{32} , one can calculate the protein adsorption, Γ , by using the protein mass balance

$$\Gamma = \frac{(C_{\text{PR}}^{\text{INI}} - C_{\text{PR}}^{\text{SER}})V_{\text{AQ}}}{SV_{\text{OIL}}} = \frac{d_{32}(C_{\text{PR}}^{\text{INI}} - C_{\text{PR}}^{\text{SER}})(1 - \Phi)}{6\Phi} \quad (3)$$

where V_{AQ} is the volume of the aqueous phase, V_{OIL} is the volume of the oil phase, $\Phi = V_{\text{OIL}}/(V_{\text{AQ}} + V_{\text{OIL}})$ is the oil volume fraction, and $C_{\text{PR}}^{\text{INI}}$ is the protein concentration in the initial solution (prior to emulsification). A more detailed description of the used experimental procedure for determination of protein adsorption is given elsewhere.¹⁵

2.5. Determination of the Size Distribution of WPC Aggregates by Dynamic Light Scattering (DLS). To determine the size of the protein aggregates (possibly containing also carbohydrate molecules) in the WPC solutions, we used a Malvern 4700 C apparatus (Malvern Instruments, Ltd., U.K.). The instrument was equipped with a K7032 CE 8-multibit 128 channel correlator, and the light source was an argon laser Innova (Coherent, USA) operating at a light wavelength of 488 nm. All measurements were performed at 27 ± 0.1 °C.

The instrument gives a histogram for the diffusion coefficients of the aggregates, D (i.e., mass % of aggregates falling in a given interval of diffusion coefficients). Then a histogram in terms of the hydrodynamic diameters, d_h , is calculated by using the Stokes-Einstein relation:

$$d_h = \frac{k_B T}{3\pi\eta D} \quad (4)$$

where $k_B T$ is the thermal energy and η is the shear viscosity of the disperse medium. Note that in the case of protein aggregates, one determines an effective diameter of the aggregates, because they are not solid spheres as assumed in eq 4.

To determine the relative fractions of the aggregates of various diameters, we filtered WPC solutions with five different filters produced by Millipore (Bedford, MA) of pore size 450 nm (type Millex HV), 220 nm (type CS), 100 nm (two filters of types VC and Millex VV) were used and showed different retention of the protein aggregates, and 50 nm (type VM). The protein concentration in the filtrates was determined by the method of Bradford.¹⁷ In parallel, the size distribution of the aggregates in the filtrates was measured by DLS. In this way, we were able to obtain a histogram, showing the relative mass of the aggregates in a given size range in the WPC solutions. No change in the

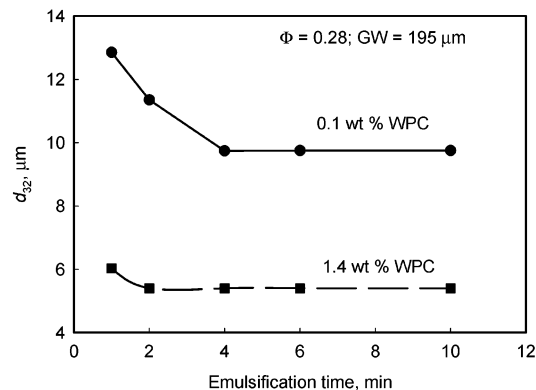


Figure 2. Surface-volume diameter, d_{32} , as a function of the emulsification time, at two different WPC concentrations, for emulsions prepared under fixed emulsification conditions: $\Phi = 0.28$, gap width of 195 μm . All solutions are at natural pH ≈ 6.2 and contain 0.15 M NaCl and 0.01 wt % Na₂S₂O₃.

average aggregate size was found by DLS upon dilution of the solutions, which indicated that the molecules in these aggregates were irreversibly attached, probably as a result of the thermal treatment applied during the production of WPC by the spray-drying method.

3. Results and Discussion

3.1. Effect of Emulsification Time on Mean Drop Size. Earlier studies,^{11,18–21} utilizing circulation mode emulsification, have shown that changes in the drop size distribution and a decrease in mean drop size occur prior to reaching a steady state. The rate for achieving the steady state depends on the hydrodynamic conditions and on the emulsifier properties (concentration, kinetics of adsorption, etc.).

To check whether the selected emulsification times, given in Table 1, are sufficient for achieving the steady drop size distribution, we performed a series of measurements of d_{32} , by taking samples from the emulsion after different periods of homogenization. As an illustration of the obtained results, we show in Figure 2 the dependence of d_{32} on the mixing time for the processing element with a gap width of 195 μm at two different WPC concentrations, 0.1 and 1.4 wt %. The results obtained with this processing element showed that d_{32} reached a steady value after ca. 4 min of emulsification for all studied concentrations. A similar dependence of d_{32} on the homogenization duration was obtained for the emulsions prepared under the other conditions studied (different gap widths, protein concentrations, and oil volume fractions). In all cases, the chosen emulsification times in Table 1 were found to exceed about 2 times the mixing duration, which was needed to reach the steady drop size distribution.

3.2. Effect of the Initial WPC Concentration on the Mean Drop Size. A series of oil-in-water emulsions was prepared by using the emulsification element with 395 μm gap width, at three different oil volume fractions, $\Phi = 0.15$, 0.28, and 0.45, at various initial WPC concentrations in the aqueous solution ($C_{\text{WPC}}^{\text{INI}}$ between 0.02 and 4.0 wt %). As an example for a typical result, the histogram

(18) Sanchez, M. C.; Berjano, M.; Guerrero, A.; Gallegos, C. Emulsification rheokinetics of nonionic surfactant-stabilized oil-in-water emulsions. *Langmuir* **2001**, *17*, 5410.

(19) Oh, S. G.; Jobalia, M.; Shah, D. O. The effect of micellar lifetime on the droplet size in emulsions. *J. Colloid Interface Sci.* **1993**, *155*, 511.

(20) Tornberg, E. Functional characterization of protein stabilized emulsions: emulsifying behaviour of proteins in a valve homogeniser. *J. Sci. Food Agric.* **1978**, *29*, 867.

(21) Tornberg, E. Functional characterization of protein stabilized emulsions: emulsifying behaviour of proteins in a sonifier. *J. Food Sci.* **1980**, *46*, 1662.

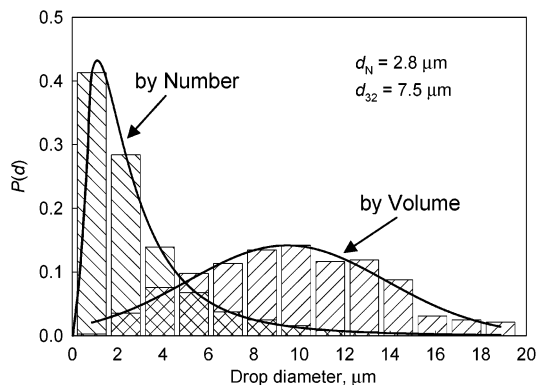


Figure 3. Histogram of the drop diameter distribution in a soybean-oil-in-water emulsion, obtained from 0.6 wt % solution of WPC (0.15 M NaCl, 0.01 wt % NaN₃, natural pH). The oil volume fraction was $\Phi = 0.28$, and the used emulsification element had a gap width of 395 μm . The number-averaged drop diameter is $d_N = 2.8 \mu\text{m}$, whereas the volume-surface diameter is $d_{32} = 7.5 \mu\text{m}$.

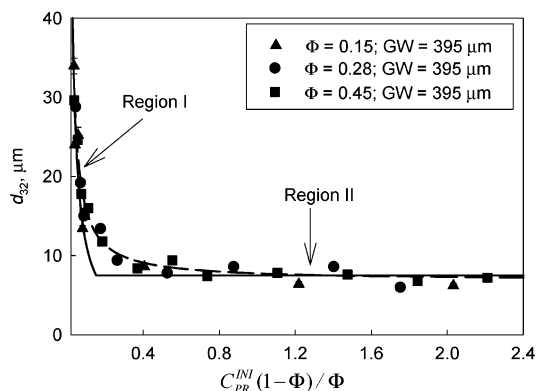


Figure 4. Surface-volume diameter, d_{32} , as a function of the normalized protein concentration for emulsions prepared at three different oil volume fractions under fixed hydrodynamic conditions (gap width of 395 μm). The points are experimental data, whereas the two continuous curves represent the calculated drop diameter in region I (eq 5) and region II (eq 7). The dashed curve represents the calculated drop diameter by means of eq 8. See the text for additional explanations.

of the drop size distribution in an emulsion with $\Phi = 0.28$ and $C_{\text{WPC}}^{\text{INI}} = 0.6 \text{ wt } \%$ is presented in Figure 3 (for comparison, both size distributions by number and by volume are shown). The number-averaged drop diameter is $d_N = 2.8 \mu\text{m}$, whereas the volume-surface diameter is $d_{32} = 7.5 \mu\text{m}$. For emulsions prepared with $C_{\text{WPC}}^{\text{INI}} > 0.4 \text{ wt } \%$, the drop size distributions were very similar to those presented in Figure 3. On the other hand, the peak of the drop size distribution was shifted toward larger diameters at $C_{\text{WPC}}^{\text{INI}} < 0.4 \text{ wt } \%$.

We found that the mean oil drop size, $d_{32}(C_{\text{PR}}^{\text{INI}})$, obtained at different oil volume fractions, Φ , can be represented by a single curve when plotted in an appropriate scale. Taking into account the difference in the area of the oil-water interface, which is created at different oil volume fractions (at equivalent mean drop size), one may plot the data for d_{32} as a function of the renormalized protein concentration, $C_{\text{PR}}^{\text{INI}}(1 - \Phi)/\Phi$: this renormalization maintains constant the ratio of the protein dissolved in the aqueous phase versus the volume of the oil phase in the emulsion (see, e.g., eq 5 below). The respective plot is shown in Figure 4 for the studied oil volume fractions (0.15, 0.28, and 0.45). As seen from Figure 4, the experimental points fall nicely on a single curve, which consists of two distinct regions: a sharp decrease

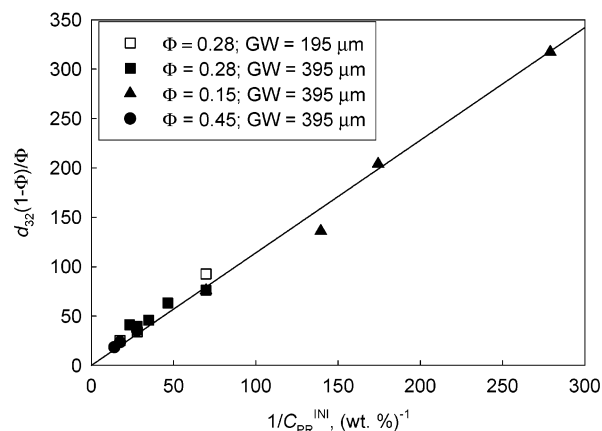


Figure 5. The normalized volume-surface diameter, $d_{32}(1 - \Phi)/\Phi$, as a function of the inverse initial protein concentration for emulsions prepared under different emulsification conditions. The line is a linear fit according to eq 5.

of d_{32} from ca. 35 μm down to 12 μm is observed in the range of normalized concentrations between 0.03 and 0.15 wt % (region I), followed by a plateau with $d_{32} \approx 7.5 \mu\text{m}$ at normalized concentrations above 0.4 wt % (region II).

The observed dependence of d_{32} on $C_{\text{PR}}^{\text{INI}}(1 - \Phi)/\Phi$ in region I can be interpreted in the following way: In this region, the observed increase of d_{32} at lower protein concentrations is certainly related to the deficiency of protein that should cover the newly created drop surface in the process of emulsification. One expects that in region I, smaller drops (as compared to those in the final emulsion at a given WPC concentration) are initially formed in the processing element of the emulsification device. However, the surface of these small drops is not covered by a sufficiently dense adsorption layer, due to deficiency of protein in the aqueous phase. As a result, an intensive recoalescence of the drops takes place within and after the processing element, so that larger drops are eventually formed in the final emulsion. In this concentration range, almost all of the protein is adsorbed on the drop surface, so that the introduction of more protein (increase of $C_{\text{PR}}^{\text{INI}}$) allows the formation of smaller drops of larger surface area.

A simple estimate of the expected drop size, at normalized protein concentrations below 0.15 wt %, can be made under the simplifying assumption that virtually all protein is adsorbed on the drop surface and that the protein adsorption corresponds to the minimal one for obtaining stable emulsions, Γ^* . Under this assumption, d_{32} can be estimated from the following expression, which represents the mass balance of the protein initially dissolved in the aqueous phase and the adsorbed protein (see eq 3 with $C_{\text{PR}}^{\text{SER}} = 0$):

$$d_{32} \approx \frac{6\Phi\Gamma^*}{(1 - \Phi)C_{\text{PR}}^{\text{INI}}} \quad (5)$$

According to eq 5, the dependence of $d_{32}(1 - \Phi)/\Phi$ versus $1/C_{\text{PR}}^{\text{INI}}$ should be a straight line with a slope, which does not depend on Φ and on the hydrodynamic conditions during emulsification. To verify eq 5, we performed an additional series of experiments with $\Phi = 0.28$, by using another processing element with gap width 195 μm (i.e., under different hydrodynamic conditions). The experimental data, obtained at different oil volume fractions and under different hydrodynamic conditions, are plotted in Figure 5, along with the best linear fit according to eq 5. Only the experimental points corresponding to $C_{\text{PR}}^{\text{INI}}(1 - \Phi)/\Phi$

– Φ)/ $\Phi < 0.15$ wt % are plotted in Figure 5, because eq 5 is expected to be a reasonable approximation only at low protein concentrations (in region I). One sees from Figure 5 that the experimental data are very well described by a straight line, and from its slope we determined $\Gamma^* = 1.9$ mg/m². The latter value is very close to the value for a dense protein monolayer, $\Gamma_M \approx 2$ mg/m² (determined as explained in section 3.3 below), which means that almost a complete adsorption monolayer should be formed on the drop surface for preventing the drop recoalescence during emulsification.

The latter result is in apparent contradiction with the reported values for the threshold surfactant adsorption, Γ^* , required for formation of emulsions, stabilized by low-molecular-mass surfactants. For instance, Taisne et al.⁶ obtained hexadecane-in-water emulsions from sodium dodecyl sulfate (SDS) solution at reported surfactant adsorption $\Gamma = 1.4 \times 10^{-2}$ mg/m², which is around 100 times lower than the value for a dense adsorption layer of SDS molecules, $\Gamma_M \approx 1.4$ mg/m². Similar results were reported by Narsimhan et al.² for tetradecane-in-water emulsions, produced by a high-pressure homogenizer in the presence of SDS. The formation of emulsions at such low surface coverage was explained by these authors as a result of electrostatic repulsion between the oil droplets² and of the Gibbs–Marangoni effect,⁶ which decelerates the drainage of the thin aqueous films between two emulsion drops (see, e.g., ref 22 for a discussion of the Gibbs–Marangoni effect in relation to film thinning). Further experiments and theoretical analysis, performed in ref 23, confirmed the importance of the electrostatic repulsion and of the Gibbs–Marangoni effect for the systems studied by Narsimhan et al.² and Taisne et al.⁶ On the other hand, the same type of analysis shows²³ that these effects are of secondary importance for the studied WPC emulsions in the presence of 0.15 M NaCl and that the drop–drop recoalescence could be prevented only when an almost dense adsorption layer is formed on the drop surface (see ref 23 for a more detailed discussion). This protein adsorption layer leads to steric repulsion between the drop surfaces and plays a decisive role in stabilizing the studied WPC systems during the process of emulsification.

For normalized concentrations above 0.4 wt % (region II, see Figure 4), the drop size remains constant, which implies that the hydrodynamic conditions during emulsification play a decisive role here (the protein is in an excess). Following the approach described by Walstra,⁴ we can explain the mean drop size in this region on the basis of Kolmogorov's theory of turbulence. According to this approach, the size of the obtained drops depends mainly on the average power density in the emulsification chamber, ϵ , which is defined as⁴

$$\epsilon = \frac{pQ}{V_{\text{DISS}}} \quad (6)$$

where p is the applied pressure difference along the emulsification element, Q is the flow rate during emulsification, and V_{DISS} is the volume of the mixing element, where the turbulent dissipation of energy takes place. For the series of experiments shown in Figure 4 (gap width of 395 μm , $\Phi = 0.28$), the power of the used equipment is

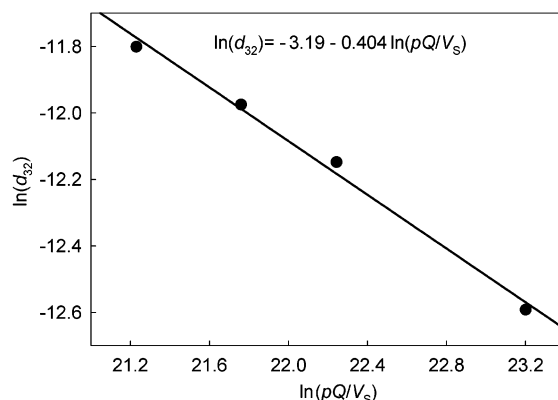


Figure 6. Logarithm of the volume-surface diameter, d_{32} , versus $\ln(pQ/V_S)$ for emulsions stabilized by 3 wt % WPC at $\Phi = 0.28$. The solid line represents the best fit used to estimate the dissipation volume, V_{DISS} .

$pQ = 28.6$ J/s. To calculate ϵ , we need to know the volume of the space where the turbulent flow is developed. In these experiments, the emulsification element consists of two consequent cylindrical slits with an external diameter of 7.34 mm and an internal diameter of 6.55 mm (see Figure 1). The length of each slit is 1.0 mm, which corresponds to a geometrical volume of the two slits $V_S \approx 17.2 \times 10^{-9}$ m³. If we use this value as an estimate of the dissipation volume in eq 6, we obtain $\epsilon \approx 1.7 \times 10^9$ J/(s·m³). Estimates of the drop diameter (viz., eq 7 below) show that this value of ϵ predicts a drop size which is significantly smaller than the one found experimentally. This means that the actual dissipation volume, V_{DISS} , is larger than the geometrical volume of the slits, V_S . This result could be anticipated, because the turbulent flow is not necessarily concentrated within the slit and could develop in a certain volume after the slit, as well. One could assume that V_{DISS} is roughly proportional to V_S . Under this assumption, one can find the respective coefficient of proportionality from the mean drop size in the emulsions obtained at high WPC concentrations, as explained below.

According to the theoretical model for emulsification in a turbulent regime,⁴ the diameter of the drops, that cannot be disrupted by the turbulent eddies, is given by the expression

$$d_K \sim \epsilon^{-0.4} \sigma^{0.6} \rho^{-0.2} \quad (7)$$

where σ is the interfacial tension and ρ is the mass density of the continuous phase. In our system, $\sigma \approx 10$ mN/m and $\rho \approx 10^3$ kg/m³. As one can see from eqs 6 and 7, the logarithm of the typical drop diameter, $\ln(d_K)$, should be a straight line as a function of $\ln(pQ/V_{\text{DISS}})$ with a slope of -0.4 . We made use of eq 7 to estimate V_{DISS} by performing emulsification experiments at high initial WPC concentration, 3 wt % (protein-rich regime), with different processing elements. The mean volume-surface diameter, d_{32} , was measured, and the plot of $\ln(d_{32})$ versus $\ln(pQ/V_S)$ was constructed; see Figure 6 (we assume $d_{32} \approx d_K$ in region II). As predicted by eq 7, the slope of the best linear fit through the experimental data was found to be very close to -0.4 and from the intercept of the straight line we estimated that $V_{\text{DISS}} \approx 10 V_S$. The latter relation is used in all further considerations to calculate the numerical values of ϵ for the used processing elements.

The position of the transition between regions I and II occurs at a certain protein concentration, which can be estimated by equilibrating d_{32} from eq 5 to d_K from eq 7

(22) Ivanov, I. B.; Dimitrov, D. S. *Thin Film Drainage*. In *Thin Liquid Films: Fundamentals and Applications*; Marcel Dekker: New York, 1988; Chapter 7.

(23) Denkov, N. D.; Tcholakova, S.; Ivanov, I. B.; Campbell, B. Emulsification and coalescence stability of emulsions. *Adv. Colloid Interface Sci.*, submitted.

(see the crossing point of the two solid curves in Figure 4). In this particular case (gap width of 395 μm), the transition is predicted at $C_{\text{PR}}^{\text{INI}}(1 - \Phi)/\Phi \approx 0.152$ wt %. One can see from Figures 4 and 5 that the experimental points comply rather well with the theoretical curve, eq 5, for normalized concentrations below 0.15 wt % (protein-poor region) and with the constant value, predicted by eq 7, for concentrations above 0.4 wt % (protein-rich region). In the intermediate concentration range, between 0.15 and 0.4 wt %, the measured drop size is slightly larger than the theoretical values calculated by both eqs 5 and 7. In this transition region, the dynamic equilibrium between drop breakage and re-coalescence leads to formation of droplets with a mean drop diameter slightly larger than d_k .

We found that the drop size dependence in the entire range of protein concentrations can be adequately described by the following empirical equation:

$$d_{32} \approx d_k + A \frac{\Phi}{(1 - \Phi)C_{\text{PR}}^{\text{INI}}} \quad (8)$$

where d_k is defined by eq 7 and A is an adjustable parameter, determined from the best fit through the experimental points. Note that eq 8 brings the essential dependence of d_{32} on the hydrodynamic conditions, protein concentration, and oil volume fraction (cf. eq 8 with eqs 5 and 7), but the adjustable parameter A has no simple physical meaning. The comparison of the experimental points with the theoretical curve corresponding to eq 8, with $A = 9$ mg/m^2 , shows an excellent agreement in the entire range of protein concentrations for all studied oil volume fractions; see the dashed curve in Figure 4.

3.3. Adsorption Isotherm of WPC. In parallel with the drop size determination, we measured the protein concentration in the serum after emulsification, which allowed us to calculate the protein adsorption on the drop surface, Γ . The obtained values are presented in Figure 7 as an adsorption isotherm $\Gamma(C_{\text{PR}}^{\text{SER}})$ for the emulsions prepared with a processing element of 395 μm gap width and $\Phi = 0.28$. One can see that the protein adsorption remained practically constant, $\Gamma = 2.0 \pm 0.2$ mg/m^2 , within the concentration range between $C_{\text{PR}}^{\text{SER}} = 0.001$ and 0.1 wt %. This constant value of Γ probably corresponds to a protein adsorption in a dense monolayer, Γ_M .

We found that Γ significantly increased at higher protein concentrations and reached 7.5 mg/m^2 at 0.8 wt % protein in the serum. The latter value of Γ is well above the value for formation of a bilayer, which is expected to be $\Gamma_{2M} \approx 2\Gamma_M \approx 4$ mg/m^2 . Such high values for WPC adsorption, $\Gamma \gg \Gamma_M$, have been already reported in the literature for WPC solutions of high concentration. For instance, Sunder et al.²⁴ reported $\Gamma = 10.5$ mg/m^2 at 0.5 wt % of whey proteins. The excess of protein adsorption over Γ_M most probably corresponds to the formation of a multilayer, which contains adsorbed protein aggregates. The mass distribution of the aggregates in the WPC solution is presented in section 3.4 below. Our attempts to fit the data in the multilayer region, $C_{\text{PR}}^{\text{SER}} > 0.13$ wt %, with the known basic adsorption isotherms (e.g., that of Brunauer–Emmett–Teller, BET) were unsuccessful. Therefore, we used an empirical equation to fit the experimental dependence $\Gamma(C_{\text{PR}}^{\text{SER}})$ in the multilayer region:

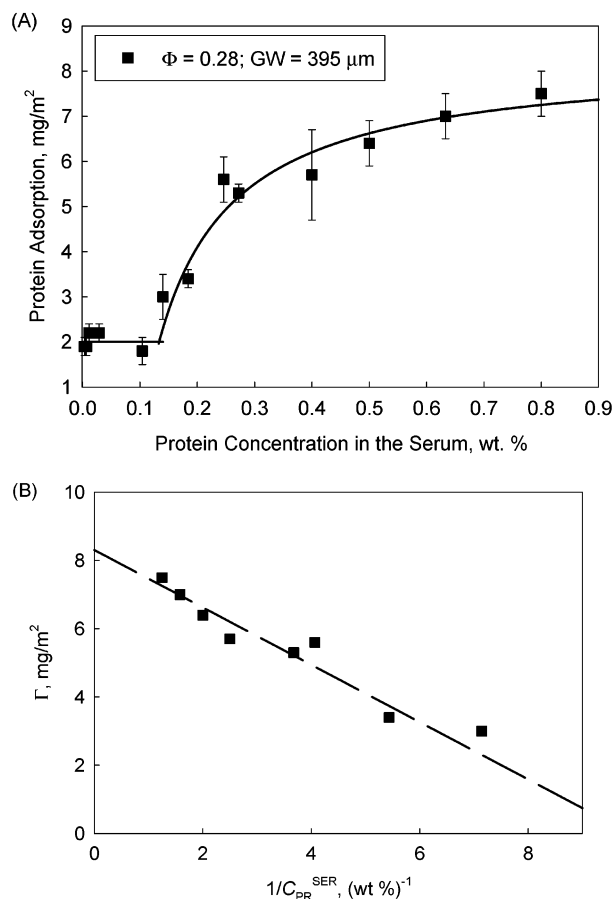


Figure 7. (A) Protein adsorption, Γ , plotted as a function of the protein concentration in the serum, $C_{\text{PR}}^{\text{SER}}$, for WPC emulsions prepared at $\Phi = 0.28$ under fixed hydrodynamic conditions (gap width of 395 μm). The points are experimental data, whereas the continuous curves represent $\Gamma = \Gamma_M = 2.0$ mg/m^2 at low protein concentrations ($0 < C_{\text{PR}}^{\text{SER}} < 0.13$ wt %) and the calculated values of Γ from eq 9 at higher protein concentrations ($0.13 < C_{\text{PR}}^{\text{SER}} < 1.0$ wt %). (B) Plot of the experimental data in the multilayer region, as a function of $1/C_{\text{PR}}^{\text{SER}}$, along with the respective linear fit according to eq 9.

$$\Gamma = 8.3 - \frac{0.84}{C_{\text{PR}}^{\text{SER}}} \quad \Gamma \geq 2 \text{ mg}/\text{m}^2 \quad (9)$$

where Γ is measured in mg/m^2 and $C_{\text{PR}}^{\text{SER}}$ is measured in wt %. As seen from Figure 7, the experimental points for $\Gamma(C_{\text{PR}}^{\text{SER}})$ are very well represented by eq 9.

Equation 9 can be used only in the region, where $\Gamma \geq \Gamma_M$, which corresponds to $C_{\text{PR}}^{\text{SER}} \geq 0.13$ wt %. After replacing $C_{\text{PR}}^{\text{SER}} = 0.13$ wt % in eq 3, one can estimate that the initial protein concentration, which corresponds to the transition from a monolayer to a multilayer, is $C_{\text{PR}}^{\text{INI}} \approx 0.19$ wt % under these conditions of emulsification (gap width of 395 μm , $\Phi = 0.28$).

3.4. Role of the Protein Aggregates in the Protein Adsorption. As mentioned in section 3.3, our attempts to fit the experimental data $\Gamma(C_{\text{PR}}^{\text{SER}})$ in the multilayer region with the basic adsorption isotherms were unsuccessful, which indicated that the adsorption multilayer most probably contained protein aggregates. The sharp onset of the multilayer formation at a certain protein concentration (see Figure 7) suggests that, probably, the first layer serves as a substrate for the adsorption of the aggregates.

To quantify the amount and the size of the protein aggregates in the used WPC solutions, we applied the

(24) Sunder, A.; Scherze, I.; Muschiolik, G. Physicochemical characteristics of oil-in-water emulsions based on whey protein–phospholipid mixtures. *Colloids Surf.* **2001**, *21*, 75.

Table 2. Size Distribution of the Aggregates in WPC Solution at Natural pH \approx 6.2, in the Presence of 0.15 M NaCl and 0.01 wt % NaN₃

	d_h , nm					
	5–15	15–165	165–190	190–225	225–450	>450
mass %	48	28	9	7	4	4

procedure described in section 2.5. We found that a significant fraction of the protein in these solutions (\approx 25%) was in the form of large aggregates with an effective diameter above 165 nm; see Table 2. If one assumes that these aggregates have fractal structure with a fractal dimension of \approx 2, one can roughly estimate that the number of protein molecules in one aggregate is of the order of $(d_h/d_p)^2 \sim 1700$ (in this estimate we used $d_h \approx 165$ nm for the hydrodynamic diameter of the aggregate and $d_p \approx 4$ nm for the diameter of the protein molecules).

To check whether the adsorption of these aggregates was related to the measured high protein adsorptions in the multilayer region, we prepared an emulsion with WPC solution, which was prefiltered through a membrane filter. The filtered solution still contained some aggregates with an effective diameter of up to \approx 200 nm, but the largest aggregates were removed (the mass fraction of the removed aggregates was about 20% from the total protein content in the initial WPC solution). The protein concentration of the filtered solution was adjusted to 0.5 wt % by dilution with an appropriate amount of electrolyte solution, and an emulsion was prepared with volume fraction $\Phi = 0.15$ by using the processing element with a gap width of 395 μ m. Measurements by the method of Bradford showed that the protein adsorption in this emulsion was significantly lower (less than 2.4 mg/m²) as compared to the adsorption in the emulsion prepared by using a nonfiltered solution of the same initial concentration of protein (\approx 6 mg/m²). This experimental result strongly supports our hypothesis that the adsorption multilayers contain a significant fraction of protein aggregates.

The protein adsorption in the first monolayer (in which the protein molecules are in direct contact with the oil–water interface) is known to be practically irreversible, because the adsorption energy per protein molecule is rather large.²⁵ On the other hand, the protein molecules adsorbed in the multilayer can be bound less strongly to the drop surface, if they are not in direct contact with the oil–water interface. Therefore, one may expect that the adsorption of protein in the multilayer region could be partially reversible and that part of the adsorbed protein (including some aggregates) could desorb upon rinsing of the emulsion with electrolyte solution.¹⁵

To check this hypothesis, we rinsed with electrolyte solution the cream formed from an emulsion prepared with 4 wt % WPC solution (for this solution we determined $\Gamma \approx 8 \pm 1$ mg/m² by the method of Bradford). The rinsing of the emulsion was performed in the following way: The emulsion was centrifuged at 1000*g* for 1 h to cream. Afterward, the serum was removed by using a syringe, and the same volume of 0.15 M NaCl and 0.1 wt % NaN₃ solution was gently introduced below the cream. The sample was gently shaken by hand until the emulsion drops were completely dispersed and then left undisturbed for 12 h. This emulsion was centrifuged again at 1000*g* for 1 h to cream, and a sample from the rinsing solution, that remained below the cream, was taken and the protein concentration was determined by the method of Bradford.¹⁷

(25) Cornec, M.; Cho, D.; Narsimhan, G. Adsorption dynamics of α -Lactalbumin and β -Lactoglobulin at air–water interfaces. *J. Colloid Interface Sci.* **1999**, *214*, 129.

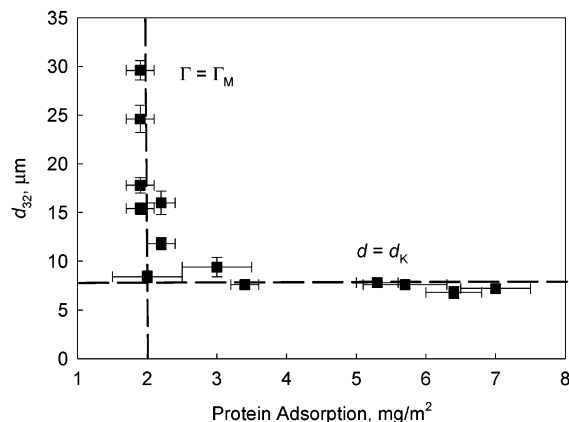


Figure 8. Mean volume-surface diameter, d_{32} , as a function of protein adsorption, Γ , for emulsions with oil volume fraction $\Phi = 0.28$, prepared by using the processing element with a gap width of 395 μ m.

The same procedure was repeated three times. The drop size distribution in the rinsed emulsions was found to be the same as that of the original emulsion; that is, no drop–drop coalescence occurred during this procedure. By using a mass balance of the protein, from the average drop diameter, d_{32} , and from the protein concentrations in the initial solution, C_{PR}^{INI} , in the serum, C_{PR}^{SER} , and in the three rinsing solutions, C_{PR}^{RIN} , we were able to calculate the protein adsorption before and after rinsing of the cream. We found that the initial adsorption of \approx 8 mg/m² decreased after the first rinsing down to \approx 6 mg/m² (protein concentration in the serum, 0.37 wt %), followed by an additional decrease of Γ after the second rinsing down to \approx 2.5 mg/m² ($C_{PR}^{SER} \approx 0.16$ wt %) and to 1.9 mg/m² after the third rinsing. Note that the latter value practically coincides with the adsorption in a monolayer, Γ_M . A similar result was obtained with emulsions formed from WPC solutions with an initial concentration of 2 and 3 wt %.

All these results indicate the following: (1) A multilayer of reversibly bound protein molecules (including aggregates) is built on the drop surface at protein concentrations above ca. 0.15 wt % in the aqueous phase. (2) The adsorption reaches a plateau at about 7–9 mg/m² at protein concentrations above ca. 0.6 wt %. (3) The protein adsorbed in an excess over the monolayer, Γ_M , is reversibly attached and can be washed out upon rinsing with electrolyte solution.

3.5. Relation between Drop Size and Protein Adsorption. The experimental results for the mean drop diameter, d_{32} , are plotted in Figure 8 as a function of the protein adsorption, Γ , for the emulsions prepared with a gap width of 395 μ m and $\Phi = 0.28$. This plot reveals two distinct regions which correspond to regions I and II in Figure 4: In the first region, Γ remains almost constant (\approx 2.0 mg/m²), whereas d_{32} decreases from 30 to 10 μ m. In the second region, the drop size remains constant, whereas Γ increases from 2 to 7.5 mg/m². In other words, the drop size is determined by the protein adsorption at low protein concentrations, whereas Γ increases at practically constant drop size at high protein concentrations.

3.6. Prediction of Protein Adsorption under Different Emulsification Conditions. From a practical viewpoint, it is important to know how the protein adsorption depends on the initial protein concentration and on the hydrodynamic conditions during emulsification. In this section, we illustrate the applicability of eqs 3, 8, and 9 for predicting the adsorption, Γ , as a function of the initial protein concentration at different oil volume

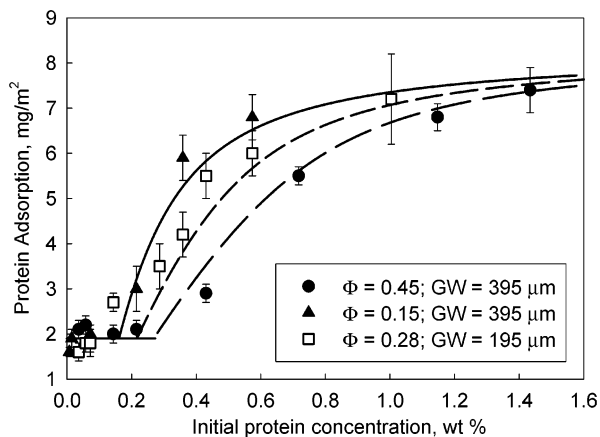


Figure 9. Protein adsorption as a function of the initial WPC concentration for emulsions prepared under different emulsification conditions. The points are experimentally measured data, whereas the curves represent the theoretical predictions according to eqs 3, 8, and 10.

fractions ($\Phi = 0.15$ and 0.45 ; gap width of $395 \mu\text{m}$) and under different hydrodynamic conditions ($\Phi = 0.28$; gap width of $195 \mu\text{m}$).

As discussed in section 3.3 above, the protein adsorption is constant, $\Gamma_M \approx 2.0 \text{ mg/m}^2$, in region I (low protein concentration). At higher initial WPC concentration, we should use the adsorption isotherm $\Gamma(C_{PR}^{SER})$ for prediction of Γ ; see eq 9. We can first calculate the protein concentration in the serum after emulsification, C_{PR}^{SER} , from the following quadratic equation, which is obtained by setting equal the protein adsorption expressed through eqs 3 and 9:

$$\frac{10(1-\Phi)d_{32}}{6\Phi}(C_{PR}^{INI} - C_{PR}^{SER}) = 8.3 - \frac{0.84}{C_{PR}^{SER}} \quad (10)$$

$$C_{PR}^{SER} \geq 0.133 \text{ wt } \% \quad \Gamma \geq 2 \text{ mg/m}^2$$

where d_{32} is determined by eq 8, and all other parameters are known. Note that a multiplier 10 has been added to the left-hand side of eq 10 (cf. with eq 3) to have the same dimensions of the quantities in both sides of the equation: d_{32} is measured in micrometers, whereas C_{PR}^{INI} and C_{PR}^{SER} are measured in wt %. From eq 10, one can calculate C_{PR}^{SER} and afterward calculate Γ from eq 9, at a given initial protein concentration, C_{PR}^{INI} .

The concentration at which the transition from a monolayer to a multilayer adsorption occurs can be calculated by replacing $\Gamma = \Gamma_M$ in eq 9, and the result reads $C_{PR}^{SER} = 0.133 \text{ wt } \%$. Replacing the latter value for C_{PR}^{SER} in eq 3, we determined that the respective initial protein concentrations (at which the transition from a monolayer to a multilayer adsorption takes place) are 0.16 or 0.26 wt % for $\Phi = 0.15$ or 0.45 , respectively (gap width of $395 \mu\text{m}$). The same procedure can be used to calculate the transition initial protein concentration for emulsions prepared under different hydrodynamic conditions. For example, one obtains $C_{PR}^{INI} \approx 0.23 \text{ wt } \%$ for the transition initial protein concentration at $\Phi = 0.28$ and a gap width of $195 \mu\text{m}$.

The comparison between the experimentally measured and theoretically calculated values of Γ is presented in Figure 9; it is seen that the agreement is satisfactory for all studied emulsification conditions, without using any adjustable parameter.

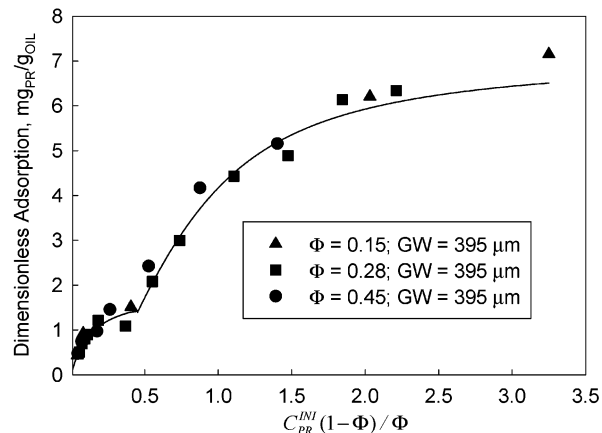


Figure 10. Dimensionless adsorption, $\bar{\Gamma}$, as a function of the normalized initial protein concentration for emulsions prepared at three different oil volume fractions under fixed hydrodynamic conditions (gap width of $395 \mu\text{m}$). The points represent experimental data, whereas the curves are calculated from eqs 8, 10, and 11.

3.7. Prediction of Other Technologically Important Parameters. In some practical applications, one can be interested in the amount of protein that is removed from the aqueous phase as a result of adsorption on the drop surface. Different quantities can be used as a measure of the efficiency of this process, depending on the particular application. From this viewpoint, one important quantity is the amount of protein retained by unit mass of the emulsified oil. The latter quantity presents a dimensionless adsorption, $\bar{\Gamma}$ [mg protein/g oil], which is defined by the following equation:

$$\bar{\Gamma} = \frac{V_{AQ}(C_{PR}^{INI} - C_{PR}^{SER})}{m_{OIL}} = \frac{6\Gamma}{d_{32}\rho_{OIL}} \quad (11)$$

where m_{OIL} is the total mass of oil in the emulsion and $\rho_{OIL} = 0.92 \text{ g/cm}^3$ is the mass density of the oil.

By using eqs 3, 8, 10, and 11, one can predict the dimensionless adsorption as a function of the initial protein concentration. The comparison between the experimental points and the theoretically calculated curves for $\bar{\Gamma}$ is presented in Figure 10 for three different oil volume fractions (gap width of $395 \mu\text{m}$), and the agreement is rather good. We found that $\bar{\Gamma}$ increases from 0.5 to 1.5 upon a 10-fold increase of the normalized protein concentration, $C_{PR}^{INI}(1-\Phi)/\Phi$, from 0.02 to 0.5 wt % (this roughly corresponds to region I in Figure 4). There is a further gradual increase of $\bar{\Gamma}$ from 1.5 to 6 at higher normalized concentrations (between 0.5 and 2 wt %), followed by a plateau with $\bar{\Gamma} \approx 6$ at even higher protein concentrations. Note that the different shapes of the curves for Γ and $\bar{\Gamma}$ (cf. Figures 9 and 10) are explained with the variation in the mean drop size; see eq 11, which shows that the dimensionless adsorption $\bar{\Gamma}$ is proportional to Γ/d_{32} . For instance, the observed initial increase of $\bar{\Gamma}$ from 0.5 to 1.1 (Figure 10) at a virtually constant value of Γ (Figure 9) is due to the observed decrease of d_{32} with the increase of WPC concentration in region I (Figure 4). The dependence of $\bar{\Gamma}$ on $C_{PR}^{INI}(1-\Phi)/\Phi$, shown in Figure 10, can be used for choosing an appropriate protein concentration, which would ensure optimal dimensionless retention, $\bar{\Gamma}$, at given remaining conditions.

Another important quantity from a practical viewpoint is the decrease of the bulk protein concentration, as a result of protein adsorption, which is defined as

$$\Delta C_{PR} = C_{PR}^{INI} - C_{PR}^{SER} \quad (12)$$

We verified the validity of eqs 8 and 10, which can be used to calculate the protein concentration in the serum after emulsification, by constructing a correlation plot for the theoretically predicted and the experimentally measured values of ΔC_{PR} . If eqs 8 and 10 describe adequately the experimental data, the points in the correlation plot should lie on a straight line with a slope equal to unity. Indeed, we found that the points in this correlation plot comply very well with a linear fit having a slope of 1.01 (correlation coefficient, 0.96). This result supports the validity of the assumptions used to derive eqs 8 and 10.

3.8. Comparison of our Experimental Results with the Results of Tornberg.^{20,21} Experiments with similar goals were performed by Tornberg^{20,21} with WPC-stabilized emulsions. The power of the valve homogenizer was varied in Tornberg's experiments to study the effect of the hydrodynamic conditions during emulsification on mean drop size and protein adsorption, whereas the initial concentration of WPC and the oil volume fraction were maintained constants ($C_{WPC}^{INI} = 2.5$ wt % and $\Phi = 0.4$, respectively). As expected, the drop size was found to decrease at higher power consumption and after a larger number of passes of the oil–water mixture through the homogenizer. The protein adsorption was found^{20,21} to decrease with the decrease of the mean drop diameter and reached a plateau value of ≈ 2 mg/m², which agrees very well with our monolayer value, Γ_M .

At a first glance, the observation of Tornberg that the adsorption becomes lower at smaller mean drop size is in apparent contradiction with part of our results; we measured higher adsorption at smaller drop size (see Figure 8). However, the way in which the drop size was changed in ref 20 was rather different from ours. In ref 20, the initial protein concentration was maintained at 2.5 wt % and a higher power density, ϵ , was applied for producing emulsions of smaller drop size. We suppose that the use of higher power densities during emulsification was accompanied with a local temperature increase in the emulsification element of the high-pressure homogenizer.^{20,21} In other words, we suppose that the reduced adsorption in ref 20 was due to heating of the emulsion while in the homogenizer valve (an increase of the sample temperature after passing through the homogenizer was indeed noticed in ref 20).

To check the above hypothesis, we performed experiments which showed that the protein adsorption in WPC-stabilized emulsions decreased after thermal treatment of the emulsions. Several emulsions, prepared at various WPC concentrations, were heated in a thermostat in the following way: The emulsion temperature was raised for 10 min from room temperature to 78 °C; then the sample was kept at 78 °C for 5 min. Afterward, the sample was taken out of the thermostat and stored for 2 h at room temperature for cooling. Finally, the serum of the emulsion was taken out and the protein concentration was determined by the Bradford method, which allowed us to calculate Γ ; see Table 3. We found that Γ was close to the monolayer value, $\Gamma_M \approx 2.0$ mg/m², for all heated emulsions (including those that correspond to a multilayer adsorption in the absence of thermal treatment). These results indicate that the protein desorbs from the multilayers upon heating. As shown in section 3.4, a fraction of the protein in the adsorption multilayer is weakly attached, and an actual protein desorption could take place at higher temperature. Therefore, the data of Tornberg^{20,21} could be explained by assuming a local heating of the emulsions

Table 3. Mean Volume-Surface Diameter, d_{32} , and Protein Adsorption, Γ , for Emulsions Preheated at 78 °C and for Nonheated Emulsions at Three Different WPC Concentrations^a

C_{WPC} , wt %	d_{32} , μm	Γ , mg/m ²	
		nonheated emulsion	preheated emulsion
0.1	11.8 \pm 0.6	2.2 \pm 0.2	2.2 \pm 0.2
0.4	7.5 \pm 0.6	3.4 \pm 0.2	2.2 \pm 0.5
0.8	7.6 \pm 0.6	5.7 \pm 0.6	2.5 \pm 0.5

^a All solutions contain 0.15 M NaCl and 0.01 wt % NaN₃.

in the emulsification device. Such a local heating is not expected to be important in our emulsification device, because we work with a much larger gap width and at lower pressure.

One could try to explain the observed²⁰ lower protein adsorption at smaller mean drop size with the reduced protein concentration in the aqueous phase; indeed, the protein adsorption on the drop surface would lead to a lower protein concentration in the aqueous phase for emulsions containing smaller drops (under equivalent other conditions). However, the protein concentration in the aqueous phase, after emulsification, was measured in ref 20. From the reported experimental data and the protein adsorption isotherm, one can estimate that the decrease of protein concentration in the aqueous phase was too small to explain the observed lower protein adsorption at smaller drop size.²⁰ Therefore, this explanation can be ruled out.

4. Conclusions

The present paper describes a systematic study of the effect of WPC concentration on drop size and protein adsorption at various oil volume fractions and hydrodynamic conditions during emulsification. The main results can be summarized as follows:

At low protein concentrations, the mean drop size is governed by a threshold value of the protein adsorption, Γ^* , which is needed for obtaining stable emulsions. Γ^* is close to the adsorption in a dense monolayer, Γ_M , and it is a characteristic of the emulsifier, which does not depend on the oil volume fraction and on the hydrodynamic conditions during emulsification. From the value of Γ^* , one can estimate the mean drop size, d_{32} , by using eq 5; see Figure 5.

At high protein concentrations, the mean drop size does not depend on the protein concentration and is determined mainly by the density power of dissipation in the emulsification device. The experimental data for d_{32} are very well described by the turbulent theory of emulsification; see eq 7 and Figure 6. In this protein-rich regime, the adsorption Γ is determined by the initial protein concentration and the mean drop size.

We find that the protein adsorption on the drop surface, Γ , is a function of the protein concentration in the aqueous phase, C_{PR}^{SER} (both measured after accomplishment of the emulsification); that is, the function $\Gamma(C_{PR}^{SER})$ can be considered as an adsorption isotherm. This result allows us to couple the equations presenting the mass balance of adsorbed and dissolved protein to the equations describing the mean drop size in an emulsion. In this way, we are able to formulate a closed set of simple equations, which predicts the mean drop size and the protein adsorption at various emulsification conditions; see eqs 6–10.

The proposed theoretical model is verified by comparing its predictions with experimental results obtained at various protein concentrations, hydrodynamic conditions,

and oil volume fractions (Figure 9). The model allows one to predict also other, technologically important quantities, such as the dimensionless protein adsorption (protein/oil) and the protein depletion from the aqueous phase as

a result of protein adsorption on the drop surface; see Figure 10.

LA034411F